Synthetic Approach to the Design of Wide-Band Microwave Injection-Locked Amplifiers

Enrico F. Calandra
Associate Professor,
D.I.E.E.T., Palermo University,
Viale delle Scenze, Ed. 9, 90128 Palermo, Italy,
e-mail: enrico.calandra@unipa.it

Daniele Lupo
PhD Student,
D.I.E.E.T., Palermo University,
Viale delle Scenze, Ed. 9, 90128 Palermo, Italy,
e-mail: daniele.lupo@unipa.it

***Abstract*— In this work, a synthesis-based approach to the realization of wide-band microwave injection-locked amplifiers (ILA) is proposed. To this purpose, a transmission-type topology is combined with a feedback structure in which the "core ILA" is intentionally separated from the output (power) amplifier. A modular, matched, design of individual building blocks of the core ILA is then adopted, which allows their first-approximation exact modeling in the dynamical complex-envelope domain, following the theory earlier developed by Calandra-Sommariva. On this basis, analytic expressions for the main operating characteristics of the ILA (such as the locking bandwidth under small signal operation) are derived in a straightforward manner. A diakoptical analysis can then be applied for the dimensioning of the free circuit parameters of each block to satisfy the overall system-level design constraints. As example of application, a DRO-based single transistor core ILA prototype operating at X-band was designed and built, showing quite satisfactory performances and agreement with stated goal specifications.**

I. INTRODUCTION

Injection-Locked Amplifiers (ILA) are adopted in a number of microwave, millimeter-wave and also opto-electronic applications [1-4]. They exploit the frequency-entrainment phenomenon occurring in a nearly-sinusoidal oscillator when driven by a monochromatic signal of appropriate amplitude and frequency. When operated in their fundamental-frequency mode (i.e., with an input signal frequency in the neighborhood of the oscillator's free-running one) they behave as saturated amplifiers or as high-power monochromatic signal sources with excellent phase noise performances [1]. The possibility of simple electronic phase-shifting of the output signal with respect to the reference one, makes them useful, e.g., for the beam-steering of phased arrays [2-4].

In all cases, the two main characterizing specs of an ILA are the injection-ratio ρ, defined as the ratio between the output power of the ILA and the injection signal power (i.e., the equivalent of the power gain of a non-saturated amplifier), and the locking band-width (LBW) achievable for any given injection-ratio value.

Unfortunately, such two quantities are conflicting each-other (a high value of ρ implies a small LBW, and vice versa) and appropriate trade-off has usually to be determined for the fulfillment of system-level specifications on the ILA.

A problem-alleviating solution was achieved in passing from the conventional reflection-type to the more modern and efficient transmission-type topologies for the implementation of the ILA circuit. In the past, the microwave and millimeter wave active devices adopted for ILA implementation have been the negative resistance diodes, and the circuit structure adopted for building an ILA was simply to add a nonreciprocal element (usually a ferrite circulator) to provide a mean to inject the driving signal and to separate it from the oscillator's output one. The pro and cons of this structure are in the fact that the oscillator can be designed in the usual way, but the injection efficiency is low and the achievable LBW is very small for reasonably high injection ratios. This can make the ILA unattractive even for the narrow band applications for which it is usually adopted. More recently, with the pervasive adoption of transistors for most low- and medium-power applications (even in the higher microwave range) the situation has changed, and the presence of separate input and output ports has permitted to adopt new circuit structures in which the ILA is designed as a whole, incorporating the injection signal mechanism into the oscillation one, in circuit configurations usually referred to as transmission-type ILA (TILA, for short, in what

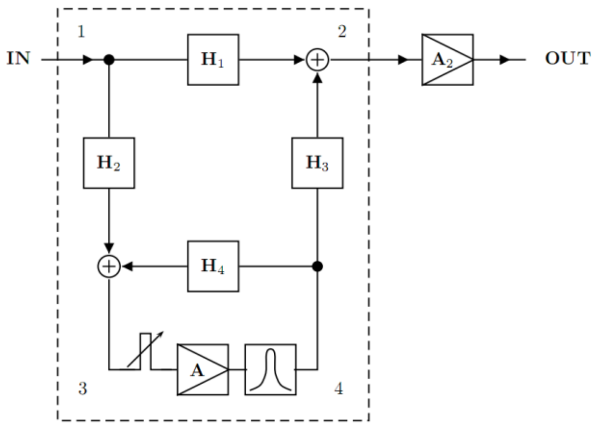

Fig.1. General block-diagram structure of a feedback-type TILA. The dashed rectangle delimits the "core TILA".

follows) [5]. Appropriately exploited, the degrees of freedom so achieved can permit to obtain much better performances for the TILA, especially in terms of wide-banding. On the other hand, the design phase is more complicated, especially when, feedback-type topologies are adopted in place of the more conventional negative-resistance ones, with a general structure which can typically be cast in the block-diagram illustrated in Fig.1.

In this connection, it has to be pointed out also that most published works on ILA deal with the specific nonlinear algorithms or simulation methods required for their analysis. The design phase is usually overlooked, and dealt with, in practice, only through empirical cut-and-try procedures. In this work, an attempt is made toward the development of a systematic and straightforward design method for the performance-driven dimensioning of the various elements of a microwave TILA with the general feedback topology of Fig.1. The proposed approach is based on the use of appropriate diakoptics of the various circuit blocks into a Z_o matched environment, and their behavioral modeling in the fundamental-frequency dynamical complex-envelope domain [6], with the help of standard circuit and E.M. simulation CAD tools. This will permit, in the end, to obtain closed-form expressions for the main TILA performances in terms of the design parameters, thus permitting their optimization as a function of system-level specifications. This goal is not easily achievable with other approaches, since determination of locking bandwidth using circuit simulators is a lengthy task, not easily automatable. Therefore, having at one's disposal an analytic expression for it, even if first-order approximate, has to be considered a great advantage and a powerful design tool.

II. Derivation of the TILA Behavioral Model

In the block diagram of the feedback-topology TILA shown in Fig.1, the generalized distribution-combining network (characterized by the transfer functions $\mathbf{H}_1$, $\mathbf{H}_2$, $\mathbf{H}_3$ and $\mathbf{H}_4$) is employed for several purposes: to ensure Barkhausen conditions to be met for stable oscillation, to inject the signal into the feedback loop, and to extract the output signal from the "core-TILA", bringing it to the output amplifier stage ($\mathbf{A}_2$) that drives the load. The reason for introducing the concept of "core-TILA" (i.e., the part of the circuit inside the dashed box) will be clearer later on, and is one of the distinguishing points of the devised design method.

In the block diagram of Fig.1, all the elements are meant to be characterized in the fundamental-frequency dynamical complex envelope domain, following the theory co-developed by one of these authors in [6]. Before proceeding, it can be remarked that the simplifications adopted for deriving the block model of Fig.1 are made here only for the sake of simplicity, and a first-order exact analysis of more complex structures could be made by proper extension of this treatment, by remaining to within the frame of the perturbation-refined theory here adopted. Of course, the basic assumption of a quasi-sinusoidal quasi-static behavior of the entrained oscillation cannot be removed, but this is not a problem in a properly dimensioned core-TILA which will certainly adopt a high-selectivity resonator to ensure the required spectral purity characteristics.

In particular, with reference to block-diagram of Fig. 1, the only element which is assumed to exhibits a significant frequency dependence to within the locking bandwidth (which is, at most, only few % of the centre-band frequency f_o) is the resonator block, which, being linear, can be characterized in terms of its scattering parameters, as also all the other linear blocks. Depending on the specific task at hand, such parameters can be derived either from measurements or, more probably, from compact circuit-models or electromagnetic simulations of the physical structures involved. As to the active element, the meant transistor amplifier in above block diagrams, it will be characterized here by its fundamental-frequency describing function [7], as detailed later on.

It can be now introduced one of the basic ideas on which relies the proposed design method, i.e., to adopt a modular approach not only in the representation, but also in the design of the various constitutive blocks. In practice, this fact can be interpreted as the requirement for all blocks to be designed as characteristic impedance Z_o matched multi-ports (typically, 50Ω). This diakoptics not only simplifies the practical design of the individual modules, but simplifies the block-interaction model of the overall core-TILA by lending itself to be cast in a behavioral nonlinear dynamical model, following the guidelines of the theory developed in [6].

According to the above consideration, we can now derive a first-approximation exact nonlinear dynamical model of the core-TILA with the feedback block structure illustrated in Fig.1, under fundamental-mode CW drive. The first step is to observe that, while the voltage and current at the output port of the core-amplifier placed after the delay line could exhibit a significant harmonic content (since working deeply into gain compression) the output of the filter will anyhow be quasi-sinusoidal because of its high-Q. Thus, both voltages at node 3 and 4 can be first-order approximated as quasi-sinusoidal quasi-static ones under transient operation. Moreover, if the intrinsic (not filtered) amplifier bandwidth is dimensioned, as reasonable, to be much wider than the filter's one, the nonlinear-wideband (amplifier) and the linear-selective (filter) blocks can be combined into a single fundamental-frequency band-limited symbolic differential model [6] of the form:

$$\mathbf{V}_4 = \mathbf{L}(D)\,\mathbf{A}(V_3)\,\mathbf{V}_3 \qquad (1)$$

Where D is the symbolic differential operator (D=d/dt), $\mathbf{A}(V_3)$ is the (phased) sinusoidal-input describing function [7] associated to the amplifying block (including the delay-line), expressed as polynomial function of the amplitude (V_3) of its driving signal phasor ($\mathbf{V}_3=V_3\ \exp\{j\phi_3\}$), calculable on the basis of a large-signal Harmonic-Balance analysis of this part of the circuit in the neighborhood of the TILA centre frequency, and L(D) is the perturbation-refined band-limited differential operator (BLDO) that characterizes the filter block in the stroboscopic time domain, as introduced in [6]. If we assume a second order modelling of the resonator, the associated BLDO turns out to be given by:

$$\mathbf{L}(D) = \mathbf{L}_0\,(\omega_o/(2Q))/(D+\omega_o/(2Q)+j\Delta\omega) \qquad (2)$$

where Q is the overall (loaded) quality factor of the feedback loop, $\Delta\omega=\omega-\omega_o$, and ω_o the resonance (angular) frequency at which the Barkhausen's phase condition is assumed to be met by proper dimensioning of the delay line length. They constitute two of the main design parameters of the core-TILA, together with L_0, H_4 and the set of coefficients defining $A(V_3)$.

Notice that the transfer function $\mathbf{H}_4$ and the coefficients of $\mathbf{A}(V_3)$, although not explicitly evidenced in the notation adopted for the sake of compactness, are not bound to be strictly constant within the locking range. A (mild) variation is allowed, provided that it does not violate the above stated assumption of a dynamics dominated, at least to the first order, by the narrow-band resonator adopted.

By combining (1) and (2) with the definition of $\mathbf{V}_3$:

$$\mathbf{V}_3 = \mathbf{H}_2\,\mathbf{V}_1 + \mathbf{H}_4\,\mathbf{V}_4 \qquad (3)$$

after some manipulation, we obtain:

$$[D+(1-\mathbf{L}_0\,\mathbf{H}_4\,\mathbf{A}(V_3))\,\omega_o/(2Q)+j\Delta\omega]V_4\exp\{j\theta_4\}= (\mathbf{L}_0\,\mathbf{H}_2\,\mathbf{A}(V_3))\,\omega_o/(2Q))\;V_1\exp\{j\theta_1\} \qquad (4)$$

Equations (3) and (4), together with the output port voltage defining equation:

$$\mathbf{V}_2 = \mathbf{H}_1\,\mathbf{V}_1 + \mathbf{H}_3\,\mathbf{V}_4 \qquad (5)$$

constitute the first-approximation exact complex envelope domain dynamical model of the of the core-TILA under examination.

Before proceeding further, it can be remarked that while node voltages are not the usual quantities adopted in microwave circuit analyses (by hand or by ECAD tools), where they are commonly replaced by wave quantities, their use is here instrumental to the derivation of the final core-TILA equations only, and they have not to be calculated or accounted for by necessity during the actual design phase.

Since we are not interested here in the transient response of the TILA but only in its steady state performances and in the LBW evaluation, we can adapt the CW regime and stability analysis developed in [6] to the dynamical model given by equations (3-5). If we limit ourselves, in this paper's context, to low-level injection operation, a secondary simplification can also be adopted and the TILA locking bandwidth can be demonstrated to be given, after appropriate calculations, by the relationship:

$$LBW_{LL} = (H_2\,V_1\,f_o)/(Q\,V_{3,osc}) \qquad (6)$$

where $V_{3,osc}$ represents the steady-state amplitude of $\mathbf{V}_3$ when the oscillator is operating under free-running conditions, given by the solution of the algebraic nonlinear equation set that can be derived from (4):

$$\mathrm{Re}\{\mathbf{L}_0\,\mathbf{H}_4\,\mathbf{A}(V_{3,osc})\}=1 \qquad (7a)$$

$$\mathrm{Im}\{\mathbf{L}_0\,\mathbf{H}_4\,\mathbf{A}(V_{3,osc})\}\,\omega_o/(2Q)=\omega_{osc}-\omega_o \qquad (7b)$$

when the Barkhausen condition on phase is satisfied around the filter centre frequency ($\omega_{osc} \approx \omega_o = 2\pi f_o$), as we assumed.

In equations (7a,b), $\mathbf{A}(V_{3,osc})$ can be interpreted as the behavioral model of the amplifier operating in nonlinear regime in the neighborhood of the angular frequency ω_o, as can be derived from a conventional Harmonic Balance simulation of the actual circuit. To this purpose, and to derive the other design quantities (H_2, Q, etc.), the adopted circuit analysis software will be probably associated to an electro-magnetic (EM) simulation tool for the proper passive filtering and coupling elements dimensioning, according to the design strategy discussed in the next paragraph.

III. TILA Design Strategy and Considerations

On the basis of the assumed diakoptics, in which all circuit stages are characterized (and, later on, designed) individually as Zo matched building blocks, the design strategy of the core-TILA is a straightforward consequence of the derived behavioral model. The analysis of relevant equations suggests some basic consideration. Firstly, to achieve a wide locking band-width for given input signal amplitude it is convenient to separate, as here done, the core amplifier required to achieve oscillating regime (via over-compensation of filter and other passive elements losses) from the final stages required to achieve the desired output power. This makes more effective the injection scheme with respect to the case in which the feedback path is derived from the actual TILA output. To this structural consideration, we can add also the practical one that there is anyhow a trade-off in the selection of the effective Q or the filter. In fact, while a low Q would ensure a wide LBW, it would also reduce the frequency stability of the free-running oscillator. As to the feedback loop losses (the term $L_0\,H_4$), it enters the LBW calculation in an indirect manner, as determining element of the intrinsic oscillation amplitude ($V_{3,osc}$) together with the coefficients of $\mathbf{A}(V_3)$, and a case by case analysis is thus required.

All these concepts can be better illustrated with reference to an actual TILA design, as done in the next section discussing the realization of an X-band DRO-based prototype designed and built our Lab.

IV. Prototype Design and Verification Measurements

The initial motivation for the development of the proposed method was to have at one's disposal a practical design tool for the implementation of non-conventional TILA topologies. In particular, the results here presented refer to a TILA configuration which does not make use of nonreciprocal elements at input port, while maintaining a reasonable value of input port return losses (which, in case of TILAs, can easily turn out to be return gains, indeed). While a discussion of this novel circuit structure and its characteristics is not of interest here (it was presented elsewhere [8]) it is a good example of application of the

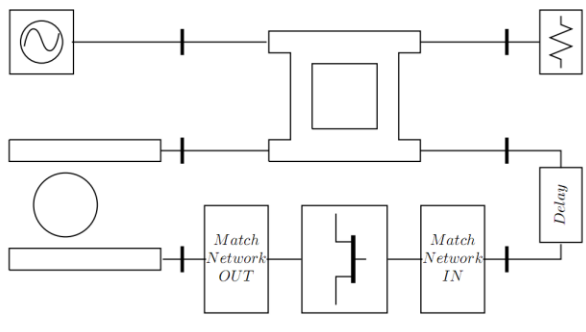

Fig.2. Circuit-diagram of the TILA prototype realized.

design method developed, and can be adopted to illustrate its practical use.

The specific circuit structure is illustrated in Fig.2. It can be noticed that the signal injection (and source isolation) is achieved via a 3dB branch-line coupler, while the filter adopts a dielectric-resonator to couple two Zo matched open ended transmission lines. This configuration possesses the adequate degrees of freedom, and permits straightforward application of the proposed design method.

The target values for the core-TILA to be designed where the center frequency (10.75GHz) and the required locking-bandwidth (>4MHz) at the nominal input signal amplitude (-20dBm).

Considering the constraints imposed by the circuit structure at hand (all centre-band values of H_n can be estimated ≈ -3dB), the product (Q $V_{4,osc}$) can be calculated and used, together with the other constraints on the feedback loop, to fix the specs for both the amplifier and the DR filter. To this purpose, firstly a single-stage amplifier has been designed (using a ATF-36077 PHEMT as active device) and behaviorally modeled. Then a number of Z_o matched DR-filters with different loaded Q (and coupling factors) have been designed with the help of EM-CAD tools, among which has been chosen the one that fitted the stated design constraints with the highest Q, while guaranteeing adequate gain margin in the feedback loop, to insure safe oscillation buildup and stability against parametric variations. The results of this procedure are concisely illustrated in Figs.3 and 4. Fig.3 shows the free-run, locked and unlocked spectra of the TILA under center-band, in-band and out-of-band operation, respectively, for the very low injection power level of -40dBm. In Fig.4 is reported instead the comparison between simulated (with this theory) and measured locking-bandwidths, exhibiting good agreement. In particular, it can be noticed the large value of 4.46MHz of locking bandwidth achieved at the target nominal operating condition of Pinj=-20dBm, to be compared to the stated goal value of 4.5MHz and to the few hundred of kHz achievable at this quite high injection ratio using more conventional design strategies.

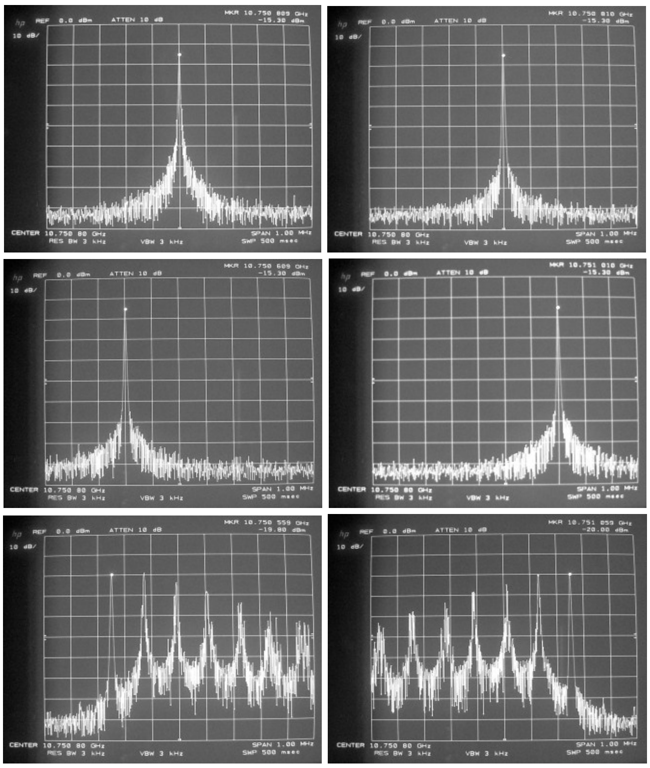

Fig.3. Measured spectra of the TILA prototype for Pinj=-40dBm.
First row: free-run and locked operation (at mid-band)
Second row: in-band locked operation (negative/positive Δω)
Third row: out-of-band unlocked operation (negative/positive Δω)

V. Conclusions

In this work a novel approach to the realization of wideband transmission-type ILA is proposed. By combining a feedback structure of the core oscillator to a modular approach for its analysis in the dynamical complex envelope domain, it permits to obtain useful analytic expressions for the main performances of the TILA. These include, in particular, an explicit formula for the locking bandwidth, which can then be used in the proper dimensioning of the TILA blocks for the fulfillment of the (usually conflicting) design specifications. Since the behavioral modeling phase of the various blocks requires use of conventional microwave circuit/EM simulation software, the proposed method lend itself as a simple and effective tool for practical TILA design problems, as demonstrated by the X-band prototype design presented.

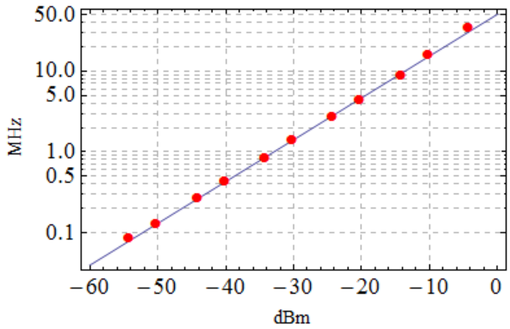

Fig.4. Simulated (line) and measured (dots) locking bandwidth of the TILA prototype vs. input power.

References

[1] K. Kurokawa: "Injection locking of microwave solid-state oscillators", *Proceedings of the IEEE*, Vol. 61, pp. 1386-1410, Oct. 1973.

[2] T. Berceli, et al.: "A double-stage injection-locked oscillator for optically fed phased array antennas", *IEEE Trans. Microwave Theory Tech.*, vol. 39, pp. 201-208, Feb. 1991.

[3] A. Daryoush, , et al.: "Phase control of optically injection locked oscillators for phased arrays", *IEEE MTT-S International Microwave Symposium Digest*, pp. 1247-1250, 8-10 May 1990.

[4] X. Zhang, A. S. Daryoush: "Full 360° phase shifting of injection-locked oscillators", *IEEE Microwave and Guided Wave Letters*, Volume 3, Issue 1, pp.14-16, Jan 1993.

[5] Y. Tajima and K. Mishima: "Transmission-type injection locking of GaAs Schottky-barrier FET oscillators", *IEEE Trans. Microwave Theory Tech.*, vol. 27, pp. 386-391, May 1979.

[6] E. F. Calandra, A. Sommariva: "Approach to the analysis of nonlinear feedback oscillators under large-signal injection", *IEE Proceedings*, vol. 133, Pt. G, No. 5, pp. 233-241, Oct. 1986.

[7] A.Gelb, W. E. Vander Velde: *Multiple-Input Describing Functions and Nonlinear System Design*, McGraw Hill, 1968.

[8] E. Calandra, D. Lupo, L. Puccio: "A DRO-based X-band Injection-Locked Amplifier Without Input Non-reciprocal Elements", *Proceedings of European Circuit Conference on Circuit Theory and Design*, Antalya, pp. 367-370, Aug. 2009.